EFFECT OF SURFACE ROUGHNESS ON THE AERODYNAMICS OF A HIGH-SPEED TRAIN SUBJECTED TO CROSSWINDS

[1]SYEDA ANAM HASHMI, [2]HASSAN HEMIDA, [3]MOHAMMAD MEHDI RASHIDI

Birmingham Centre for Railway Research and Education, School of Civil Engineering,
University of Birmingham, United Kingdom

Abstract - Most trains have irregular surfaces or parts attached to their bodies that can be represented as roughness in general. However, irregularities, which may exist on train surfaces have normally been ignored in previous studies concerned with train aerodynamics. Therefore, for the first time, this work investigates the effects of roughness on the overall pressure distribution on a train body subjected to crosswinds. This research was aimed onto providing an understanding of the aerodynamics of a 1:25 model-scale passenger train subjected to crosswinds, both with and without surface roughness. Roughness was applied to the roof of the train surface in the form of longitudinal strips, where the height and width of these strips was 1 mm and 2 mm, respectively. The research findings revealed that the roughness on the roof surface was able to reduce the surface pressure on the roof and leeside of the train. It was also observed that the roughness with a 0.7% relative size (the height of roughness/the height of train) was able to change the surface pressures on the roof up to a maximum of 59%. Overall, it was concluded that the rough roof surface could agitate the wind flow in a complex manner.

Keywords- Crosswinds, Pressure coefficients, Rough Surface, Smooth surface, Wind Tunnel tests, Train Aerodynamics.

I. INTRODUCTION

High-speed trains are known to play an important role in public transportation around the world and are supported by the European Union, China, Korea, and France (Ryder, 2012). Since train bodies serve for a long period of time, their geometric features must be chosen carefully. As Diedrichs (2003) discussed, designing high-speed trains to be lighter and longer is the current aim in the optimisation of railway vehicles. This is done mainly to ensure savings in travel times. However, this results in potential risks for the train bodies. A train body subjected to crosswinds is surrounded by a complex flow field. This may lead to steady and unsteady aerodynamic forces acting on the vehicle. Derailment or even overturning of trains is plausible under the action of strong crosswinds (Hashmi et al., 2019). To improve the safety of trains, a number of measures have been realised. These include design improvements made with the aim of improving the external aerodynamics of the train bodies. Such design improvements include ensuring low centre of gravity for the trains, avoiding protruding objects on the roofs, large roof radii corners, sufficiently low external roof heights, favourable cross-sections, and streamlined front ends (Diedrichs, 2003). In fact, Browand et al. (2009) mentioned in their study that design factors may have a strong influence on the stability of train bodies. Therefore, assessment of crosswind stability of high-speed trains with different design features is an important subject. To do so, experimental studies on train aerodynamic properties under the action of crosswinds can help in understanding the flow around a train body and its associated aerodynamic forces and moments. Therefore, detailed investigation on the impacts of crosswinds may lead to key findings, which can help provide solutions to reduce the risk of derailment or overturning of high-speed trains (Hashmi et al., 2019). European standards suggest some important requirements and test procedures for crosswind assessments of railway vehicles (EC, 2008; RSSB, 2009; CEN, 2018). EN 14067-1 and BS EN 14067-6 are amongst the several standards which present details about methods for assessing train stability in crosswinds through various tests such as full-scale, model-scale and numerical. Also, one of the important parameters for assessment of trains in crosswinds is the angle of wind attack.

A number of experimental as well as numerical studies have investigated the aerodynamic response of trains under the impact of crosswinds (Cooper, 1979; Schulte-Werning and Matschke, 1997; Hemida and Krajnovic, 2010; Baker et al., 2011; Dorigatti et al., 2015; Hashmi et al., 2019). To elaborate, these works considered the various factors which can have an influence on the stability of a train in strong crosswinds with varying yaw angles. For instance, Hemida and Krajnovic (2010) performed a numerical study to explore the influence of the shape of a train nose on the flow structures, which develop around trains, under varying yaw angles. In their study, they performed numerical simulations on train models with either a long nose or a short nose. The results from their study showed that the short nose model resulted in highly unsteady and three-dimensional flows around the nose. These flows were found to yield more vortices in the wake as compared to the long nose train model. Therefore, the study concluded that comparatively, the short nose not only influenced the surface flow but also had an impact on the dominating frequencies. These resulted from the flow instabilities in the shear layer. Another study by Cheli et al. (2010) investigated experimentally the influence of infrastructure scenarios on the aerodynamic loads

acting on a train body. In their study, they made use of the ETR500 train and considered different infrastructure scenarios: embankment, viaduct and flat ground with and without ballast and rail. The study was able to highlight the influence of the different infrastructure scenarios on the aerodynamic loads. Furthermore, Hashmi et al. (2019) studied the aerodynamic performance of a passenger train with and without different shapes of windbreak walls, under varying yaw angles, inside a wind tunnel. The results from the study showed clear differences in terms of pressure distribution around the train surface with the use of all types of windbreak walls in the windward side, as compared to cases without any use of a windbreak wall.

While these recent works provided noteworthy insights on train aerodynamic properties for different test cases, most of these studies did not consider the effects of roughness on train surfaces of the aerodynamic forces. Roughness in this context refers to an irregularity, which may occur on the surface of the train due to a geometric feature. Therefore, the works performed in the past have usually considered smooth train surfaces by often ignoring some details in the geometry of train bodies. This is usually done in experimental tests to ease the process of constructing a scaled model. Whereas, in numerical works, it might be practically difficult to reproduce an exact replication of the full-scale model and often some unnecessary details may be simplified to create ease in meshing the geometry and performing numerical simulations. In reality, most trains have external protruding objects fitted to their bodies. These may include exterior cameras or train indicator lights. While these can be expected to have a minor or even negligible influence on the flows around trains and the safety of the trains, these may be ignored. However, certain objects fitted on the train exteriors may have an influence on the flow around the train. For instance, certain trains have pleated structures on the roof to reinforce strength to the train body while some trains have rain cover eaves to prevent water deposition. These geometric features can be expected to influence the flow fields around trains and can have a considerable effect on the stability of the formed boundary layers on train surfaces. In fact, it can be anticipated that such external structures can result in various flow separations and reattachments and thus lead to changes in the aerodynamic forces experienced by train surfaces.

Miao and Gao (2015) numerically investigated the influence of ribs on the aerodynamic performance of a train. In their study, they made use of the detached eddy simulation (DES) to numerically solve the flow around a generic train model with and without different ribs. In their study, they made use of convex ribs and cutting ribs where the former referred to upward protrusions while the latter referred to the downward cuttings. The ribs were devised in a uniform manner on the roof of the train. The results from their study revealed that the use of convex ribs was able to change the resulting lift force coefficient of the train from negative to positive, when compared to the case with no ribs. In addition, the overall overturning moment was observed to increase considerably as well with the use of both kinds of ribs. The study concluded that ribs on train surfaces could agitate the flow fields and the flow structures present around trains, thus contributing to flow separation on the roof of the train. They also stated that some sort of air suction is possible due to both kind of ribs with complex vortices developing on the leeward side of the train as compared to the case with no ribs. Overall, while the results presented by Miao and Gao's (2015) are quite interesting, they lack accurate validation data from wind tunnel tests or similar. As Dorigatti et al. (2015) discussed, numerical simulations do play a key role in the evaluation of train performances but are not yet considered sufficient in terms of accuracy for designing purposes (EC, 2008; RSSB, 2009; CEN, 2018). Therefore, experimental techniques are known to be the most widely used option in terms of accuracy as well as time.

As detailed above, not much data is presented in the literature, which examines the aerodynamic response of trains with irregular surfaces, specifically in an experimental manner. Therefore, it is important that the concept of irregular train surfaces is investigated experimentally in order to better understand how such surfaces can affect the flow around a train subjected to crosswinds. This paper presents the analysis of the results obtained from an experimental campaign carried out at the University of Birmingham's Wind Tunnel facility. The research was aimed onto providing an understanding of the surface pressures on a 1:25 model-scale passenger train subjected to crosswinds, both with and without irregular roof surfaces. Section 2 explains the experimental methodology adopted in this research while providing a detailed description of the wind profile in the wind tunnel. Section 3 provides the results of the experimental work with a discussion of the findings while Section 4 concludes the research by listing the main research outcomes along with providing suggestions for future work.

II. WIND TUNNEL CHARACTERISTICS AND THE EXPERIMENTAL SETUP

A. Wind Tunnel Facility

The experimental work in this research was performed at the University of Birmingham's (UoB) wind tunnel facility. The wind tunnel has a cross-sectional area of 2 m by 2 m and has a 10 m long working test section. 49 axial fans are used to provide the required wind

flow at the inlet of the wind tunnel through a honeycomb screen, which allows the provision of a uniform wind speed with minimum turbulence. For measuring the three-dimensional flow velocities, a Series 100 Cobra probe with 2 kHz (TFI, 2011) was used. Prior to any experimental work, characteristics of the flow inside the wind tunnel were determined.

Fig. 1 (a) shows the vertical wind profile (VWP) for the streamwise ($\overline{U}$), lateral ($\overline{V}$) and vertical ($\overline{W}$) mean velocities, respectively, at a height of 0.35 m from the floor of the wind tunnel. Fig. 1 (b) illustrates the streamwise turbulence intensity inside the wind tunnel. It must be noted that these profiles were measured without any models at the exact place where the train model was located in the experimental runs. As discussed in Hashmi et al. (2019), the presence of a splitter plate does not modify the wind speed profile, especially in the section where the train model was placed. Based on the horizontal wind profile measurements, the spanwise average of the streamwise mean velocities (u) was considered as 7.2 m/s. The average streamwise turbulence intensity is 5.5 %, as shown in Fig. 1b.

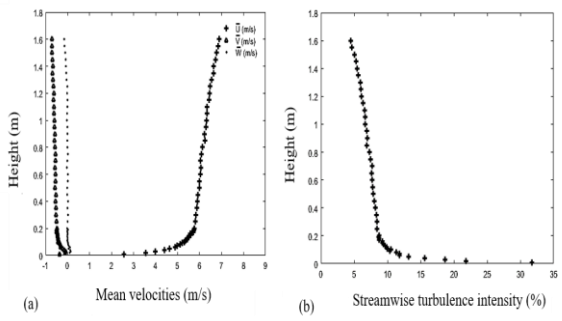


Fig. 1. Vertical wind profile (VWP); (a) streamwise ($\overline{U}$), lateral ($\overline{V}$) and vertical ($\overline{W}$) mean velocity components and (b) streamwise turbulence intensity at the centre of the wind tunnel.

B. Scaled models and experimental set-up

As noted in Section 1 of this paper, this work aims to investigate the effect of surface roughness on the aerodynamic flow around a train body. To do so, experiments were performed on a smooth train surface and a rough train surface, for comparison purposes. The experiments were performed at a yaw angle of 90°. To represent surface roughness, longitudinal strips of PVC material were used in a pleated manner on the roof of the train. The overall length of the train model was 1.5 m, where the first car was 1 m long. The height and the width of the train model was 0.156 m and 0.110 m, respectively. Experimental investigation was carried out on only the first car and the partial leading car was used for providing a realistic flow (CEN, 2018). In terms of the ground scenario, a Single Track and Ballast Rail (STBR) was adopted. For the experiments, the wind tunnel testing section consisted of a splitter plate, positioned at 6 m from the inlet of the wind tunnel. The splitter plate was used to negate the effects of boundary layer and the high turbulence intensity formed near the ground, as shown in Fig. 1. Thus, the splitter plate was located at a height of 300 mm from the wind tunnel floor. As shown in Fig. 2, the 1:25th scale model of the Class 390 Pendolino train was placed on top of a STBR, mounted on top of the splitter plate.

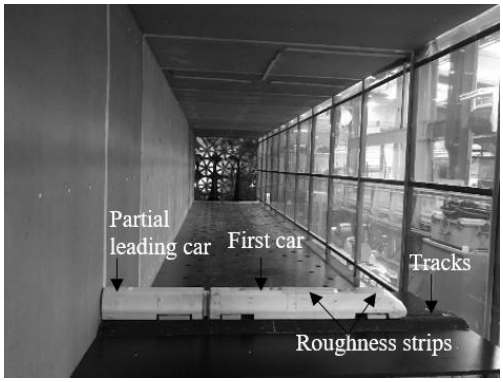


Fig. 2. The experimental set-up of the train model at a yaw angle of 90° inside the wind tunnel.

The first car was equipped with a 162 pressure taps, assembled in a series of 14 loops (A-N) in a longitudinal direction of the train, as shown in Fig. 2 (a). The pressure taps were connected to a 500 Hz multi-channel, Digital Pressure Measurement System (DPMS) with the use of PVC tubings. The DPMS allows for measuring the surface pressures on scaled models. Fig. 3 illustrates the coordinate system used with reference to the onset wind. The longitudinal position of each loop is shown where L is the first car's total length, i.e. is 1 m.

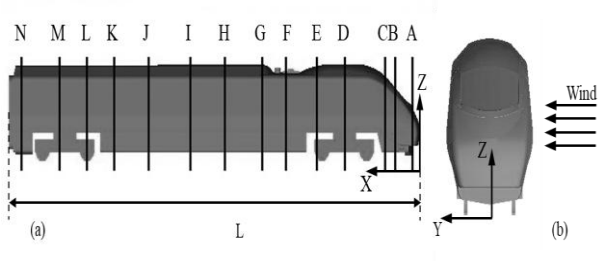


Fig. 3. (a) Position of the loops and (b) Coordinate system with reference to onset wind.

C. Test cases

Two experiments were conducted in this study, which are listed below:

(a) Train with smooth surface at a yaw angle of 90°
(b) Train with a rough surface at a yaw angle of 90°

For the experiments concerning rough surfaces, PVC strips with height and width of 1 mm and 2 mm, respectively, were glued on the roof of the train in a longitudinal direction of the train length in a pleated manner. As illustrated in Fig. 4a, loops D, E, G, H and I were under the influence of these roughness strips. Fig. 4b shows the roof of a typical high-speed train with a rough surface.

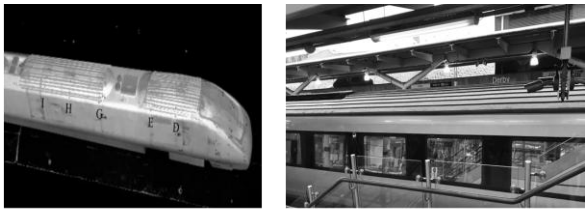


Fig. 4. (a) Demonstration of the added roughness strips and their respective positions in terms of the loops D, E, G, H and I. (b) Roof of a typical high-speed train with a rough surface.

III. RESULTS AND DISCUSSION

A. Mean pressure coefficients

For measuring the surface pressures, a 64-channel data logger with a frequency of 500 Hz was used. The mean pressure for a single pressure tap was obtained by time averaging the instantaneous data that had been collected, for a period of three minutes. The pressure distribution results obtained over the train surface for the experiments at a yaw angle of 90° can be expressed in terms of a non-dimensional pressure coefficient, C_P:

$$C_P = \frac{P - P_O}{0.5\rho V_{ref}^{\ 2}} \qquad (1)$$

where P, P_O, ρ and $V_{ref}^{\ 2}$ are the actual surface pressure at a single pressure tap, the reference pressure, the air density and the reference velocity of the wind in relation to the train, respectively.

For both the experimental tests, loops A to N were investigated where loop A is located at the nose of the train and loop N is situated at the tail of the train. Each loop represented a cross-section of the train and can be split into four sections: the windward side (WWS), the roof (ROOF), the leeward side (LWS) and the underbody (UB). This section represents the results of surface pressure in a polar coordinate form, as shown in Fig. 5.

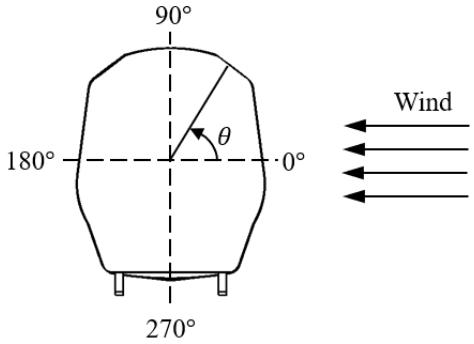


Fig. 5. Orientation of angle θ with respect to onset wind (Hashmi et al., 2019).

B. Train with a smooth surface at a yaw angle of 90°

The main aim of this research was to investigate the effect of a rough train surface on the flow which forms around a train body. However, prior to that, it was important to first obtain data for a train model with a smooth surface. Such a case would act as a benchmark and would then assist in demonstrating the intensity of the change in the results obtained.

Fig. 6-9 illustrate the mean surface pressure coefficient distribution at loops D, E, G and H for the smooth train surface at a yaw angle of 90°. Based on the results achieved in these figures, it is apparent that the WWS of the model usually demonstrated the highest-pressure trends. As the wind impinges directly on the train surface, stagnation regions develop on the WWS. In fact, such a trend is noticeable on almost all loops, which demonstrate positive pressure on the WWS of the train. Next, as the flow transits from the WWS to the ROOF, the positive pressure values can be seen to decrease significantly. This is mainly due to a large suction taking place because of the flow acceleration on the windward edges of the roof. Over the roof of the model, the flow tends to demonstrate weaker suctions due to flow separations. In terms of the LWS, where the wake of the flow exists, uniform C_P can be observed. As noted above, while the WWS tends to demonstrate strong positive pressure peaks, the ROOF as well as the LWS of the model tend to result in negative pressures, thus indicating suctions. One interesting finding details that the flow usually starts to stabilise from the middle of the ROOF to the LWS. This indicates the possible flow reattachment following flow separations.

C. Train with a rough surface at a yaw angle of 90°

As mentioned in section 2, roughness was introduced on the roof of the train in the form of longitudinal strips, arranged in a pleater manner. As a result, loops D, E, G, H and I were under the influence of these strips. Therefore, this section intends to mainly discuss the C_P distribution achieved on the loops D, E, G, H and I.

In terms of the results obtained with both the surfaces, it is apparent that the trend followed by the C_P distribution around the train body was quite similar for both the cases. However, as expected there were slight differences in the magnitude of C_P obtained. Generally, for all loops (A-N), most of the windward regions demonstrated positive C_P results with negative values obtained for regions with flow accelerations. Furthermore, as the flow transits from the WWS to the ROOF, the C_P values tend to decrease, indicating flow accelerations.

Fig. 6 illustrates the mean surface pressure distribution on loop D for the two cases examined. In terms of the WWS, this is the surface where the flow is expected to impinge directly. The surface pressure in this region

tend to be quite similar, comparatively as can be seen in Fig. 6. This could mainly be due to no roughness present on the WWS. However, as the flow progresses towards the roof, there are apparent differences in the results obtained in the C_p obtained for the two cases. While a decrease in the C_p values is noticeable for both the cases as the flow transits from the WWS to the ROOF, the effect of roughness is evident. The introduction of roughness on the roof of the train results in much lower C_p values, indicating strong suctions, as compared to the C_p results obtained with a smooth roof surface. To elaborate, at θ = 55.3°, the flow is in a transition region from the WWS to the ROOF. The windward edge of the roof has a major influence on the flow, indicating flow accelerations. For the smooth surface of the train, the C_p results demonstrated a strong suction peak. However, with the rough roof surface, a stronger suction is evident, comparatively. In terms of the flow that exists on the roof, it is apparent that the rough surface results in an overall lower C_p distribution (i.e. larger negative values are obtained) as compared to the results achieved with a smooth roof surface. One interesting finding lies at θ = 70°, where the addition of roughness seems to not have an influence in the results obtained for both cases. Another interesting finding is that while for the smooth surface it can be observed that the flow stabilises from somewhat the middle of the roof all the way to the LWS, this is not exactly the case for the flow which develops with the rough surface. To elaborate, for the rough surface, from the middle of the roof, the C_p results tend to increase thus showing pressure gradients before the flow stabilises in the LWS.

Furthermore, in order to better comprehend the influence of a rough roof surface on the flow which exists around a train body, the relative difference for each pressure tap can be calculated. Hence, in this study, the relative difference (RD) is defined by:

$$RD = \frac{\overline{C_{P\,Rough}} - \overline{C_{P\,Smooth}}}{\overline{C_{P\,Smooth}}} \times 100 \quad (2)$$

Where $\overline{C_{P\,Rough}}$ and $\overline{C_{P\,Smooth}}$ are the mean non-dimensional pressure coefficients for each tap with a rough roof surface and smooth roof surface, respectively.

For loop D, a relative difference between the two cases examined is quite visible with a maximum value of 59% for the pressure tap located at θ = 80°, which corresponds to a pressure tap located close to the middle of the roof. Such a *RD* clearly indicates the influence of the roughness strips on the pressure distribution around the train body. In addition, from the results, a smooth roof surface presents a laminar boundary layer. However, with the addition of roughness strips, the surface encounters a turbulent boundary layer.

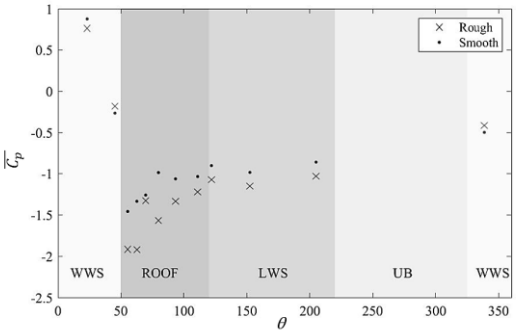


Fig. 6. Comparison of the mean surface pressure coefficient distribution at loop D for the rough and smooth train surfaces at a yaw angle of 90°.

Quite similarly, for loops E and G, as shown in Fig. 7 and Fig. 8, the C_p distribution for the rough roof surface presented overall lower values as compared to the values obtained with the smooth roof surface. However, the trend adopted by the C_p distribution over the roof of the train is slightly different as compared to loop D. To elaborate, while a noticeable relative difference is apparent between the results of the smooth and rough roof surfaces, the maximum *RD* for loop E was observed at θ = 58° with a value of 45.8%. The position of the corresponding pressure tap was close to the windward edge of the roof. This was also the case in loop G. One reason behind this finding could be due to the overall geometry of the train where the roof of the train has different geometric curvatures at different cross-sections. Also, as demonstrated in Fig. 4, loop D was somewhere in the middle of the area covered by the strips. Whereas, loop E was located towards the end of the longitudinal strips and loop G was located at the beginning of the second set of longitudinal strips.

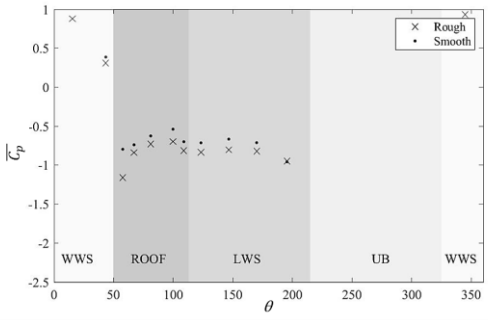


Fig. 7. Comparison of the mean surface pressure coefficient distribution at loop E for the rough and smooth train surfaces at a yaw angle of 90°.

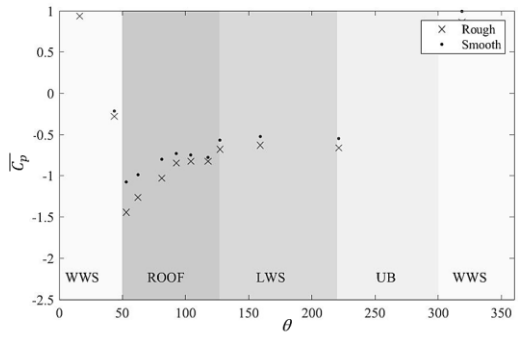


Fig. 8. Comparison of the mean surface pressure coefficient distribution at loop G for the rough and smooth train surfaces at a yaw angle of 90°.

In terms of loop H, a slightly different trend was observed in the achieved C_p distribution compared to other loops for the two cases examined. The results obtained on loop H in terms of C_p distribution are illustrated in Fig. 9. The strong suction peak observed at θ = 53° remained. However, on this loop, the wind flow seemed to be agitated in a much more complex manner as compared to other loops. Also, as seen in other loops where the rough-roof surface usually resulted in overall lower C_p distribution, this was not the case for this loop. For this loop, mainly on the roof, lower C_p values with a smooth roof surface can be observed at certain pressure taps. An increase along with fluctuations in surface pressures with the rough surfaces is evident.

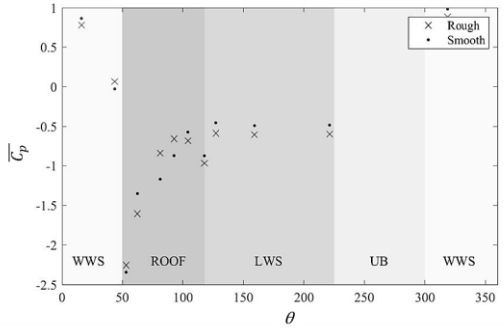


Fig. 9. Comparison of the mean surface pressure coefficient distribution at loop H for the rough and smooth train surfaces at a yaw angle of 90°.

IV. CONCLUSION

For the first time, this work experimentally investigates the effects of roughness on the overall pressure distribution on a train body subjected to crosswinds. To do so, experiments were conducted on a train body with a smooth roof surface and a rough roof surface at a yaw angle of 90°. The following conclusions could be drawn from the results of this study:

- Overall, despite the height of the added roughness with respect to the train height being less than 0.7%, it appears that the strips have an influence on the overall pressure distribution around the train, with mainly differences seen in the roof and leeward regions.
- For most of the loops, it was evident that the C_p values on the roof of the train were lower for the rough roof surface as compared to the smooth roof surface.
- An increase along with fluctuations in surface pressures with the rough surfaces is evident thus implying the agitation of the wind flow due to the roughness strips.
- Considerable relative differences between the smooth and rough roof surfaces were evident in terms of the pressure distribution results with the maximum *RD* being 59%.

ACKNOWLEDGEMENTS

The work was financed by a University of Birmingham (UK) funded scholarship and was supported by the EU H2020 project LiftTRAIN (701693).

DECLARATION OF CONFLICTING INTERESTS

The author(s) declared no potential conflicts of interest with respect to the research, authorship, and/or publication of this article.

REFERENCES

[1] Baker, C., Hemida H., Iwnicki, S., Xie, G., Ongaro, D., 2011. Special issue: The integration of crosswind forces into train dynamic modelling. Proceedings of the Institution of Mechanical Engineers. Part F J. Rail Rapid Transit. 225 (2), 154-164.

[2] Browand, F., Ross, J., McCallen, R., 2009. The Aerodynamics of Heavy Vehicles II: Trucks, Buses, and Trains. Berlin.

[3] CEN, 2018. Railway applications - Aerodynamics - Part 6: Requirements and test procedure for cross wind assessment. PrEN 14067–6 2009-02. CEN/TC 256.

[4] Cheli, F., Corradi, R., Rocchi, D., Tomasini, G., Maestrini, E., 2010. Wind tunnel tests on train scale models to investigate the effect of infrastructure scenario. J. Wind Eng. Ind. Aerod. 98, 353-362.

[5] Cooper, R., 1979. The probability of trains overturning in high winds. In: Proceedings of the 5th International Conference on Wind Engineering, Fort Collins. 2, 1185-1194.

[6] Diedrichs, B., 2003. On computational fluid dynamics modelling of crosswind effects for high-speed rolling stock. Proceedings of the Institution of Mechanical Engineers. Part F J. Rail Rapid Transit. 217 (3), 203-226.

[7] Dorigatti, F., Sterling, M., Baker, C., Quinn, A., 2015. Crosswind effects on the stability of a model passenger train - A comparison of static and moving experiments. J. Wind Eng. Ind. Aerod. 138, 36-51.

[8] EC, 2008. TSI—technical specification for Interoperability of the trans-European high-speed rail system, 'rolling stock' sub-system, TSI-HS2008/232/EC. Off. J. Eur. Union.

[9] Hashmi, S.A., Hemida, H. and Soper, D. 2019. Wind tunnel testing on a train model subjected to crosswinds with different

windbreak walls. Journal of Wind Engineering and Industrial Aerodynamics. 195.
[10] https://doi.org/10.1016/j.jweia.2019.104013.
[11] Hemida, H., Krajnovic, S., 2010. LES study of the influence of the nose shape and yaw angles on flow structures around trains. J. Wind Eng. Ind. Aerod. 98, 34-46.
[12] Miao, X. and Gao, G. (2015). Influence of ribs on train aerodynamic performances. Journal of Central South University, 22(5), pp.1986-1993.
[13] RSSB, 2009. Resistance of Railway Vehicles to Roll-Over in Gales, Railway Group Standard GM/RT 2142. Rail Safety and Standards Board Ltd.
[14] Ryder, A., 2012. High speed rail. Journal of Transport Geography, 22, 303-305.
[15] Schulte-Werning, B., Matschke, G., 1997. Measures and strategies to minimise the effect of strong crosswinds on high speed trains, Proceedings of the WCRR World Congress of Railway Research, Florence, Italy. vol. E. 569–575.
[16] TFI, 2011. Turbulent Flow Instrumentation - Cobra Probe - Getting started guide. Technical report.

★★★